Sn diffusion during Ni germanide growth on $Ge_{1-x}Sn_x$

J. Demeulemeester,[1, a)] A. Schrauwen,[2] O. Nakatsuka,[2] S. Zaima,[3] M. Adachi,[3] Y. Shimura,[3] C.M. Comrie,[3] C. Fleischmann,[4] C. Detavernier,[4] K. Temst,[4] and A. Vantomme[4]

[1)] *Instituut voor Kern- en Stralingsfysica and INPAC, K.U.Leuven, Celestijnenlaan 200D, B-3001 Leuven, Belgium*

[2)] *Graduate School of Engineering, Nagoya University, Furo-cho, Chikusa-ku, Nagoya 464-8603, Japan*

[3)] *Department of Physics, University of Cape Town, Rondebosch 7700, South Africa*

[4)] *Department of Solid State Sciences, Ghent University, 9000 Gent, Belgium*

In this paper, we report on the redistribution of Sn during Ni germanide formation on $Ge_{1-x}Sn_x$/<Ge(100)> and its influence on the thin film growth and properties. These results show that the reaction involves the formation of Ni_5Ge_3 and NiGe. Sn redistributes homogenously in both phases, in which the Sn/Ge ratio retains the ratio of the as-deposited $Ge_{1-x}Sn_x$ film. Sn continues to diffuse out of the NiGe and $Ge_{1-x}Sn_x$ after full NiGe formation and segregates in two regions: (i) at the interface between the germanide and $Ge_{1-x}Sn_x$ and (ii) at the surface, which has major implications for the thin film and contact properties.

[a)] e-mail: jelle.demeulemeester@fys.kuleuven.be

In order to boost the ever-improving performance of complementary metal-oxide-semiconductor (CMOS) devices, major research efforts are being made to enhance the charge carrier mobility in the semiconductor channel area. Strain engineering of the channel area by embedded source/drain stressors offers an elegant solution to tailor the ballistic hole and electron velocities.[1] Si-based CMOS-technology with $Si_{1-x}Ge_x$ and $Si_{1-x}C_x$ source/drain stressors, creating uniaxial compressive stress in the pMOSFET and tensile strain in the nMOSFET channel respectively, even outperforms the charge transport properties of bulk-Ge. The same strategy can be used to increase the ballistic hole and electron velocity in Ge by applying embedded $Ge_{1-x}Sn_x$ and $Ge_{1-x}Si_x$ source/drain stressors, respectively. However, the addition of Sn to the Ge matrix raises a number of challenges yet to be dealt with. (i) The solubility of Sn in Ge is limited to 1 at. % in a bulk solid solution,[2] whereas at least 5 at. % Sn (or 1 GPa uniaxial compressive stress) has to be incorporated in the matrix to outperform Si-based stressor technology.[3] Although Sn concentrations far above 5 at. % can be reached by molecular beam epitaxy (MBE), fast high-throughput growth of $Ge_{1-x}Sn_x$/Ge substrates by e.g. chemical vapor deposition or sputter deposition is not yet accomplished. (ii) Source/drain electrodes are ideally formed by solid phase reaction of a thin metal layer with the substrate. Hence, it is crucial to gain profound insight in the influence of Sn on the solid phase reaction and properties of the germanide thin film. Previous work shows that Sn segregates at the $Ge_{1-x}Sn_x$ surface at temperatures relevant for contact formation, indicating that the Sn redistribution during the growth will be a key parameter in understanding this ternary solid phaser reaction.[4] Ni being an excellent candidate for contact formation on Ge,[5,6] we therefore investigated the phase formation and atomic diffusion during the Ni germanide growth.

A 120 nm thick $Ge_{1-x}Sn_x$ layer with 8.6 at.% Sn was grown by MBE deposition on a cleaned Ge(100) substrate. X-ray diffraction 2-dimensional reciprocal space mapping confirmed that the Sn atoms are located on substitutional lattice sites and that no Sn segregation occurs during deposition. A 50 nm thick Ni film was subsequently sputter-deposited at room temperature to obtain a sample structure of 50 nm Ni/ 120 nm $Ge_{0.91}Sn_{0.09}$/ <Ge(100)>. As such, full transformation of Ni into $NiGe_{1-x}Sn_x$ leaves 15 nm of $Ge_{1-x}Sn_x$ unreacted. The phase sequence and the atomic diffusion were probed *in situ* during the solid phase reaction by real-time x-ray diffraction (XRD) and real-time Rutherford backscattering spectrometry (RBS), respectively. The main advantage over the conventional *cook-and-look* approach is

that the risk of overlooking transient but crucial stages during the reaction is minimized. Moreover, the continuous probing allows to disentangle the dynamic interplay between the redistribution of the additives, the phase formation and the diffusion kinetics.

The germanide phase formation was monitored by real-time (XRD) at a ramp rate of 0.5 °C/s from 20 °C to 850 °C in He atmosphere. Data were collected every 2 seconds, using a Cu K_α source and a linear detector covering 20° in 2θ-range. This measurement is displayed as a contour plot in Fig. 1, which allows one to deduce the phase sequence and the evolution of the crystalline quality. The x-axis represents the temperature, the diffraction angles are indicated on the y-axis, whereas the diffraction intensity is represented by a (logarithmic) color scale.

The atomic diffusion of the three constituents (Ni, Ge and Sn) was probed by real-time RBS at a ramp rate of 2 °C/min. RBS is an ion beam technique which is fully quantitative in composition and depth.[7] Real-time RBS, *i.e.* the successive acquisition of RBS spectra at a periodic time interval during a thermal treatment, thus allows to monitor the atomic diffusion quantitatively as a function of the annealing sequence.[8] The energy of the He^+ beam was set at 2.7 MeV in order to resolve the Sn signal throughout the full reaction (i.e. avoid overlap with the Ge signal), and thus enables unambiguous analysis of the Sn redistribution. All spectra were successively collected every 2 min by two ruggedized detectors at backscattering angles of + 165° and - 165°, respectively, while the sample normal was tilted by 20° in a plane defined by the incident beam and the two detectors. The simultaneously acquired spectra were analyzed with NDF in a consistent way for both detectors.[9] The contour map shown in Fig. 2 is constructed by plotting the RBS spectra from consecutive measurements (one detector only) during the temperature ramp-up one after the other. The backscattering energy can be read from the x-axis, the temperature is indicated on the y-axis and a color scale represents the backscattering yield. Element-specific depth scales, ranging from the surface towards the interior of the sample, are indicated for the sake of clarity. Due to the small difference in mass between Ni and Ge, both RBS signals overlap at backscattering energies below 2.061 MeV. Consequently, it is not straightforward to obtain a qualitative overview of the Ni germanide phase formation merely by visual inspection, which is often feasible for more simple systems.[10] The Sn signal, however, is well isolated, which allows to deduce the Sn redistribution during Ni germanide growth. It should be noted that the temperature scales of both real-time techniques can not be compared directly due to the

difference in the ramp rates applied (imposed by the difference in required data collection time).

Despite the different ramp rates, both techniques reveal the same phase sequence, similar to the growth of Ni germanide on Ge(100).[6,11] The first phase to grow is Ni_5Ge_3, which is soon followed by the growth of NiGe as evidenced by the appearing set of diffraction peaks at 290 °C (see Fig. 1). Unlike most thin film diffusion couples, here two phases grow *simultaneously*. This can be inferred from the fact that the Ni, the Ni_5Ge_3 and the NiGe diffraction peaks are all present during this stages of the reaction up to a temperature of 310 °C, where the Ni peak disappears (see Fig. 1). The Ni germanide growth is represented in the real-time RBS measurement by the bending of the Ni and Ge contours from approximately 200°C up to 300 °C (Fig. 2). RBS confirms the findings from the real-time XRD data. Metallization is initiated by the growth of a thin layer of Ni-rich germanide, which is soon followed by the formation of NiGe and the continued simultaneous growth. Analysis of the RBS spectra shows that simultaneous germanide growth occurs in separate layers in the following depth profile: $Ni/Ni_5Ge_3/NiGe/Ge_{1-x}Sn_x$. As soon as the Ni is completely consumed, NiGe continues to grow at the expense of Ni_5Ge_3. NiGe is the thermodynamically stable and final Ni germanide phase in this system.

The redistribution of the Sn content during germanide growth can be deduced from the backscattering signal between 2.22 and 2.4 MeV in the real-time RBS measurement (Fig. 2). Three spectra, acquired at different stages during the reaction (i.e. as-deposited, 290 °C and 450 °C) are displayed in Fig. 3 to clarify the Sn redistribution process. The RBS spectrum taken at room temperature (open circles) shows that the Sn content was spread homogeneously throughout the $Ge_{1-x}Sn_x$ layer. No Sn redistribution or segregation was observed prior to the germanide formation (i.e. up to 200 °C). The simultaneous bending of the Ge, Ni and Sn contours in the real-time RBS contour plot (Fig. 2) indicates that the Sn redistribution is triggered by the start of the Ni germanide formation. As Ni reacts with the $Ge_{1-x}Sn_x$ layer to form Ni_5Ge_3, Sn is incorporated in that Ni_5Ge_3 layer; i.e. $Ni_5(Ge_{1-x}Sn_x)_3$. Moreover, the Ge/Sn ratio in the Ni germanide layer retains the value of the Ge/Sn ratio in the $Ge_{1-x}Sn_x$ film (i.e. 1/0.086). Firstly, this indicates that Sn is soluble in the Ni rich germanide phase at these concentrations. Earlier work on bulk Ni-Ge-Sn ternary systems also showed that Ni_5Ge_3 and Ni_3Sn_2 can form a continuous solid solution up to the melting point.[12] However, our measurements could not reveal how Sn was incorporated in the Ni rich

germanide layer (i.e. substituting Ge in Ni_5Ge_3, segregated at the Ni_5Ge_3 grain boundaries, or as Ni_3Sn_2 dissolved in Ni_5Ge_3). Secondly, this indicates that Ni is probably the dominant diffusing species, similar to the case of Ni_5Ge_3 growth in binary Ni/Ge diffusion couples. Indeed, if Ge were the diffusing species, a much larger variation in the Ge/Sn ratio would be expected due to a difference in diffusivity between Ge and Sn.

Similar to the case of $Ni_5(Ge_{1-x}Sn_x)_3$ growth, the Sn/Ge ratio in the $NiGe_{1-x}Sn_x$ layer remains equal to ratio of the substrate (i.e. 1/0.086). One should keep in mind that NiGe is formed via two processes: (i) the dissociation of $Ni_5Ge_3 \rightarrow$ 3 NiGe + 2 Ni and (ii) the reaction between the released Ni and Ge from the substrate 2 Ni + 2 Ge $\rightarrow$ 2 NiGe. Hence, the Sn fraction (or the Sn/Ge ration) in the $NiGe_{1-x}Sn_x$ layer formed via dissociation is inherited from its precursor, the Ni rich layer, which explains why the Ge/Sn ration remains constant. The Sn fraction incorporated in the $NiGe_{1-x}Sn_x$ formed via reaction (ii), has to originate from the $Ge_{1-x}Sn_x$ substrate. After full transformation into $NiGe_{1-x}Sn_x$ the Sn content is spread homogenously throughout the full $NiGe_{1-x}Sn_x$ film at a Ge/Sn ratio similar to the one of the initial $Ge_{1-x}Sn_x$ film. This is further illustrated in figure 3 by the spectrum taken at the end of the $NiGe_{1-x}Sn_x$ formation (at 290 °C). The nearly horizontal Sn signal represents the homogeneous distribution of Sn in the $NiGe_{1-x}Sn_x$ layer from the interface to the surface.

Although no solubility issues were encountered during $NiGe_{1-x}Sn_x$ growth, the continued evolution in the Sn real-time RBS contours above 290 °C shows that the Sn redistribution does not come to a halt once the $NiGe_{1-x}Sn_x$ formation is completed. Analysis clearly reveals that Sn enrichment occurs at (i) the interface between $NiGe_{1-x}Sn_x$ and the remaining $Ge_{1-x}Sn_x$ and (ii) at the surface. This can be deduced from the emerging bumps at the low and high energy edges of the Sn signal in the real-time RBS surface plot after the completion of the $NiGe_{1-x}Sn_x$ formation (at 290 °C) and at higher temperatures (see Fig. 2 and 3). The real-time RBS plot shows that the Sn content at those locations continues to increase upon annealing. RBS cannot distinguish between Sn segregation at the surface and an increased amount of Sn incorporated in the $NiGe_{1-x}Sn_x$ surface region. In real-time XRD, on the other hand, a new diffraction peak emerges at 470 °C (after the completion of the $NiGe_{1-x}Sn_x$ growth) at a diffraction angle of $2\theta = 39$ °. This peak matches the Sn (220) diffraction peak and cannot be linked to any Ni germanide or ternary phase. Moreover, optical microscope images taken from a specimen quenched at 550 °C (i.e. with that diffraction peak being

present) clearly reveal the presence of droplets at the surface (see inset of Fig. 1). This suggests that the presence of a $NiGe_{1-x}Sn_x$ layer could not prevent the segregation of Sn at the surface. Whether the interface contains segregated Sn as well, or merely a Sn enrichment of the $Ge_{1-x}Sn_x$-near-interface region cannot be concluded from these data. RBS further shows that the Sn enrichment at those locations is at the expense of Sn in the $NiGe_{1-x}Sn_x$ layer and Sn in the $Ge_{1-x}Sn_x$ layer. The Sn concentration in the $NiGe_{1-x}Sn_x$ layer decreases from 8 at. % to 5 at.% relative to Ge at 450 °C, whereas the Sn profile in the unreacted $Ge_{1-x}Sn_x$ layer becomes more shallow and more concentrated at the $NiGe_{1-x}Sn_x/Ge_{1-x}Sn_x$ interface.

The real-time XRD plot shows that further annealing to elevated temperatures causes severe changes in the film crystallinity. At 620 °C the diffraction peak of Sn disappears suggesting melting of the segregated Sn. In correlation to this event, the diffraction peaks of the Ni germanide exhibit a significant decrease in intensity. Optical microscope images of a specimen quenched at 650 °C indicate that agglomeration of the germanide layer occurred above 620 °C (inset Fig. 1). The fact that the melting temperature (and consequently the $NiGe_{1-x}Sn_x$ agglomeration temperature) is higher than for bulk Sn, could be related to size effects and the influence of the underlaying germanide.

Our results indicate that Sn exerts a significant influence on the germanide thin film properties. On the other hand, the effects on the growth in terms of phase sequence and growth kinetics seem to be rather limited. Similar to Ni germanide growth, the first phase to grow is $Ni_5(Ge_{1-x}Sn_x)_3$ followed by a simultaneous growth of the latter phase with $NiGe_{1-x}Sn_x$ and finally a full transformation in $NiGe_{1-x}Sn_x$. We attribute this to the absence of extreme redistribution features such as the segregation of a Sn diffusion barrier and the low driving force to form ternary or binary phases with Sn. Additionally, the low melting point of Sn suggests a high mobility of Sn for diffusion in solids. Sn is thus not expected to form a huge impediment to the diffusing atoms. This results in the observed homogenous Sn distribution in both germanide phases, during the growth. Although not further investigated in this work, this Sn incorporation in the growing phases may significantly influence other properties such as the germanide texture, stress evolution and consequently the electronic and mechanical properties of the film. An important result is that the Sn segregation, usually observed in bare $Ge_{1-x}Sn_x$ substrates at temperatures above 420 °C, is not prevented by the presence of a $NiGe_{1-x}Sn_x$ capping layer. Moreover, Sn is found to enrich the $NiGe_{1-x}Sn_x/Ge_{1-x}Sn_x$

interface and to segregate at the $NiGe_{1-x}Sn_x$ surface. First, this enhances the agglomeration of the $NiGe_{1-x}Sn_x$ film at elevated temperatures (compared to NiGe films on Ge(100)),[6] deteriorating the electrical properties of the contact. Second, draining Sn from the unreacted $Ge_{1-x}Sn_x$ influences the stress on the Ge channel. This may result in a decrease of the electron - hole velocities in the Ge channel, jeopardizing the desired enhancement of electrical transport.

In conclusion, the phase sequence and growth kinetics of Ni germanide growth are relatively unaffected by the presence of Sn. Ni-rich germanide and $NiGe_{1-x}Sn_x$ are observed to grow simultaneously, with $NiGe_{1-x}Sn_x$ being the final phase. Sn however, continues to redistribute after the germanide formation, which has a significant influence on the thin film properties. Sn segregates at the $NiGe_{1-x}Sn_x$ interface and surface, which promotes the agglomeration of the thin film. As such, other metal germanide thin films preventing the segregation of Sn might be more suitable to form contacts in strained-Ge CMOS technology.

This work was supported by FWO, GOA/2009/006, CREA/07/005, INPAC EF/05/005 and IAP P6/42 in Belgium, the FWO (Flanders)/JSPS (Japan) bilateral programs, and the NRF in South Africa. The authors also thank the Material Research Group at iThemba LABS for the use of their facilities and F. Seidel for the microscope imaging.

REFERENCES

[1]D. A. Antoniadis and A. Khakifirooz, IEDM Technol. Dig. (2008).

[2]H. Stöhr and W. Klemm, Z. Anorgan. Allg. Chemie **241**, 305 (1939).

[3]B. Vincent, Y. Shimura, S. Takeuchi, T. Nishimura, G. Eneman, A. Firrincieli, J. Demeulemeester, A. Vantomme, T. Clarysse, O. Nakatsuka, S. Zaima, J. Dekoster, M. Caymax, and R. Loo, Microelectron. Eng. **88**, 342 (2011).

[4]T. Nishimura, O. Nakatsuka, Y. Shimura, S. Takeuchi, B. Vincent, A. Vantomme, J. Dekoster, M. Caymax, R. Loo, and S. Zaima, Solid-State Electron. **60**, 46 (2011).

[5]S. Gaudet, C. Detavernier, A. J. Kellock, P. Desjardins, and C. Lavoie, J. Vac. Sci. Technol., A **24**, 474 (2006).

[6]S. Gaudet, C. Detavernier, C. Lavoie, and P. Desjardins, J. Appl. Phys. **100**, 034306 (2006).

[7]W.-K. Chu, J. W. Mayer, and M.-A. Nicolet, *Backscattering Spectrometry*, Chu1978 (Academic Press, New York, 1978).

[8]J. Demeulemeester, D. Smeets, N. P. Barradas, C. M. Comrie, A. Vieira, K. Temst, and A. Vantomme, Nucl. Instr. and Meth. B **268**, 1676 (2010).

[9]N. P. Barradas, C. Jeynes, and R. P. Webb, Appl. Phys. Lett. **71**, 291 (1997).

[10]J. Demeulemeester, D. Smeets, C. Van Bockstael, C. Detavernier, C. M. Comrie, N. P. Barradas, A. Vieira, and A. Vantomme, Appl. Phys. Lett. **93**, 261912 (2008).

[11]C. Perrin, D. Mangelinck, F. Nemouchi, J. Labar, C. Lavoie, C. Bergman, and P. Gas, Meter. Sci. Eng., B **154-155**, 163 (2008).

[12]K. Wang, A. Nishikata, Y. Mishima, and T. Suzuki, Z. Metallkd. **81**, 905 (1990).

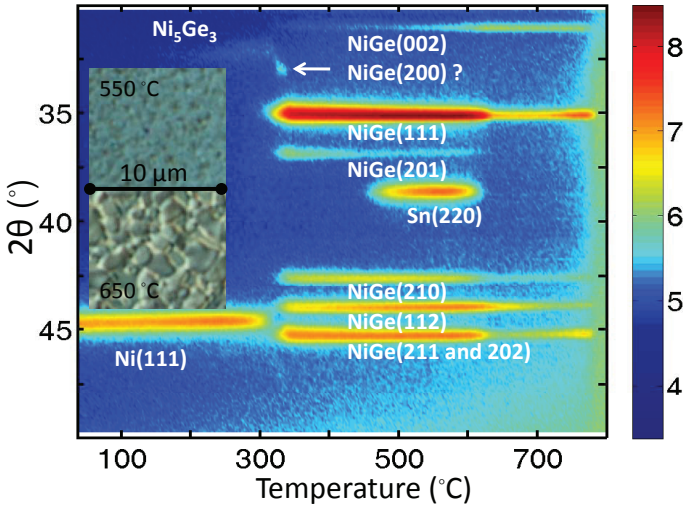

FIG. 1. (color online) Contour plot of a real-time XRD measurement probing the phase formation of Ni with $Ge_{1-x}Sn_x$ during a ramped annealing at 0.5 °C/s. The insets display microscope images of quenches taken at 550 and 650 °C.

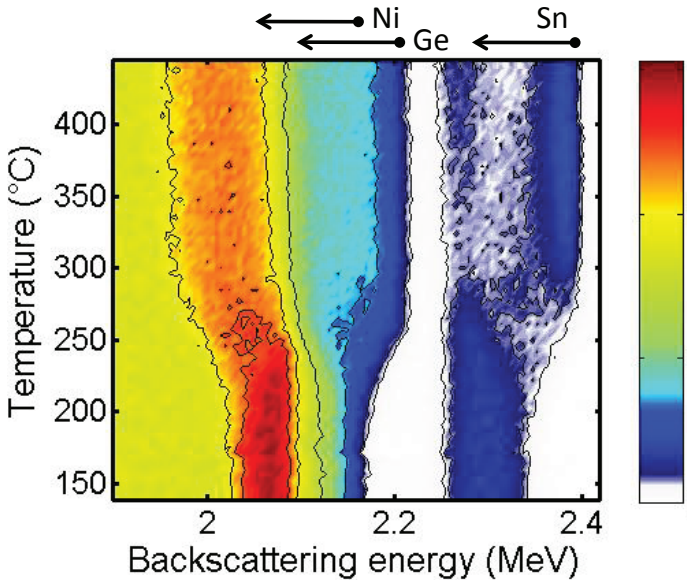

FIG. 2. (color online) Contour plot of a real-time RBS measurement probing the solid phase reaction of Ni with $Ge_{1-x}Sn_x$ during a ramped annealing at 2 °C/min. The arrows represent the element-specific depth scales, pointing from the the sample surface towards the interior of the sample.

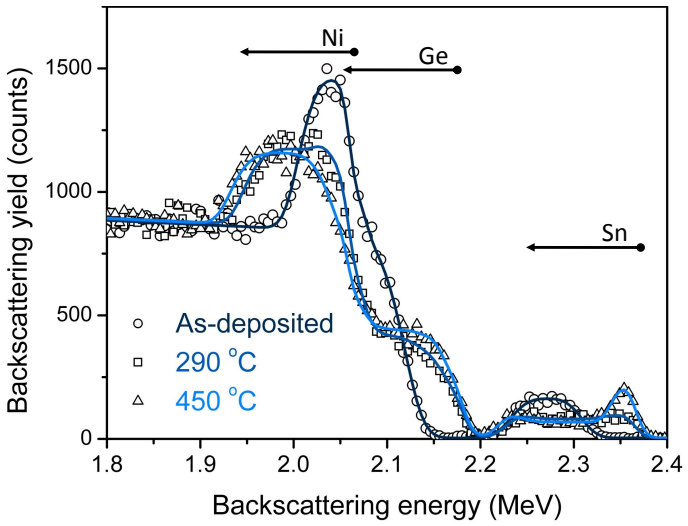

FIG. 3. (color online) Overview of 3 RBS spectra isolated from the real-time RBS measurement at room temperature (circles), 290 °C (squares) and at 450 °C (triangles) The solid lines represent the fit to the data. Indicative elemental depth scales are added for the sake of clarity.